The Journal of Prevention of Alzheimer's Disease 12 (2025) 100264

Contents lists available at ScienceDirect

The Journal of Prevention of Alzheimer's Disease

journal homepage: www.elsevier.com/locate/tjpad

Brief Report

A modelling approach to derive population-specific cutoff for plasma p-Tau217

Tau Ming Liew[a,b,c,d,*], for the Alzheimer's Disease Neuroimaging Initiative[1]

[a] Department of Psychiatry, Singapore General Hospital, Outram Road, Singapore 169608
[b] SingHealth Duke-NUS Medicine Academic Clinical Programme, Duke-NUS Medical School, 8 College Road, Singapore 169857
[c] Health Services and Systems Research, Duke-NUS Medical School, 8 College Road, Singapore 169857
[d] Saw Swee Hock School of Public Health, National University of Singapore, 12 Science Drive 2,#10-01, Singapore 117549

ARTICLE INFO

Key words:
Plasma biomarkers
Alzheimer's disease
Optimal cutoff
p-Tau217/Aβ42 ratio
Lower- and middle-income countries

ABSTRACT

Plasma pTau-217 shows promise for detecting Alzheimer's disease, but needs population-specific cutoffs for effective use. Conventional cutoff determination relies on invasive or costly gold-standards, limiting scalability. This study evaluated Finite Mixture Modelling (FMM) for establishing cutoffs without gold-standards. FMM was applied to derive cutoffs for Lumipulse plasma p-Tau217 and p-Tau217/Aβ42 ratio among 1039 ADNI participants, with validation conducted in a subset with amyloid PET data (n = 711). Additionally, simulations were conducted to determine the minimum sample size for reliable FMM estimation. The results showed that FMM-derived cutoffs effectively classified participants into brain amyloid-negative, -positive, and -indeterminate groups, with an indeterminate proportion <20 %, negative and positive predictive values near or above 90 %, and with p-Tau217/Aβ42 outperforming p-Tau217. These FMM-derived cutoffs demonstrated test performance that surpassed several previously-established cutoffs, including the recent FDA-approved cutoff. At least 900 samples were needed for reliable cutoff estimation. In conclusion, this study demonstrated the effectiveness of a modelling approach for estimating plasma p-Tau217 cutoffs without reliance on gold-standards. This approach simplifies the determinating of population-specific cutoffs and facilitates adoption of plasma p-Tau217 in communities lacking access to gold-standards, including some LMICs.

Background

Alzheimer's disease (AD) is an age-related neurodegenerative disorder and the leading cause of dementia globally. It is characterized by brain accumulation of amyloid-beta plaques and neurofibrillary tangles containing hyperphosphorylated tau, which results in progressive cognitive decline [1]. Early and accurate diagnosis of AD is crucial for effective intervention, especially with emerging disease-modifying therapies that target these pathological hallmarks [1–3]. Traditionally, cerebrospinal fluid (CSF) and positron emission tomography (PET) have been the gold standards for detecting AD pathology [1,4]. However, these methods are either invasive or costly, limiting their scalability in community settings [4–6]. Recent advancements have highlighted the potential of plasma biomarkers as more accessible and cost-effective alternatives for AD diagnosis. Plasma phosphorylated tau (p-Tau), especially p-Tau217 and p-Tau217/Aβ42 ratio, have shown promising accuracy in detecting brain amyloid [6–15]. Compared to CSF and PET, these plasma biomarkers are non-invasive and less costly, making them appealing for widespread research and clinical use [4,5]. These cumulative evidence has also led to the most recent FDA (Food and Drug Administration) approval of plasma p-Tau217/Aβ42 ratio on the Lumipulse platform [16] – a fully automated chemiluminescence enzyme immunoassay platform that enables standardized, high-throughput biomarker quantification [17,18].

However, before plasma p-Tau217 can be broadly implemented, its optimal cutoff must be determined to ensure accurate interpretation [4]. Particularly, the cutoffs may need to be customized to each distinct population, considering that the biomarker levels can be affected by demographic factors (e.g. ethnicity, body mass index, chronic kidney disease) [4,5,19], and cutoffs from one population may not generalize to another [10]. Conventionally, cutoffs of plasma biomarkers are determined using Receiver Operating Characteristic (ROC) curve analysis, which iden-

* Corresponding author at: Department of Psychiatry, Singapore General Hospital, Outram Road, Singapore 169608.
E-mail address: liew.tau.ming@singhealth.com.sg

[1] Data used in preparation of this article were obtained from the Alzheimer's Disease Neuroimaging Initiative (ADNI) database (adni.loni.usc.edu). As such, the investigators within the ADNI contributed to the design and implementation of ADNI and/or provided data but did not participate in analysis or writing of this report. A complete listing of ADNI investigators can be found at: http://adni.loni.usc.edu/wp-content/uploads/how_to_apply/ADNI_Acknowledgement_List.pdf

https://doi.org/10.1016/j.tjpad.2025.100264
Received 21 May 2025; Received in revised form 18 June 2025; Accepted 25 June 2025

tifies points that maximize sensitivity and specificity, typically using CSF or PET as a gold standard [6]. While effective, this method is more feasible in tertiary specialist centres with advanced facilities and less practical in community settings due to logistical and financial constraints [5,6]. Furthermore, access to gold standards is often limited to specific subpopulations that differ distinctly from the general population [4,5]. As an example, in the current study, participants with amyloid PET data differed significantly from those without (e.g. more likely to be younger, female and cognitively unimpaired; as seen in Supplementary Material 3), potentially introducing bias and reducing generalizability when deriving optimal cutoffs from these selective subpopulations with available gold standard data.

To overcome reliance on gold standards, recent literature proposes Finite Mixture Modelling (FMM) as an alternative approach, leveraging biomarker data alone to estimate cutoffs (i.e. without relying on gold standards e.g. amyloid PET) [20,21]. FMM has proven effective in determining cutoffs for other blood biomarkers, such as C-reactive protein [20], and in the field of AD, FMM-derived cutoffs for CSF Aβ42 have shown improved predictive accuracy for disease progression [21]. FMM operates by assuming data arises from a mix of underlying distributions representing different subpopulations [20,21]. By estimating these distributions' parameters, FMM can classify individuals into subpopulations without the need to reference to any gold standards.

Although promising, FMM is relatively nascent in the field of AD biomarkers. Its validity is not yet proven definitively. Using a large sample from the Alzheimer's Disease Neuroimaging Initiative (ADNI), this study evaluated the utility of FMM in establishing optimal cutoffs for Lumipulse plasma p-Tau217 and p-Tau217/Aβ42 ratio. Specifically, the study aimed to:

1) Derive optimal cutoffs using FMM (i.e. without relying on any gold standards);
2) Validate the performance of FMM-derived cutoffs in determining amyloid PET positivity, within a smaller subset of participants with available amyloid PET data.

Essentially, this study sought to demonstrate that cutoffs for plasma p-Tau217 can be accurately estimated without gold standards, using FMM alone. By doing so, it aimed to provide a simplified methodology for determining population-specific reference intervals [4,5], thus facilitating accurate results interpretation and encouraging widespread adoption of plasma p-Tau217 in community settings and lower- and middle-income countries (LMICs) where gold standards may not be available for cutoff determination.

Methods

Study population

The study included 1039 participants with available data on plasma p-Tau217 and p-Tau217/Aβ42 ratio from ADNI database (adni.loni.usc.edu; downloaded on 25th February 2025). ADNI is a public-private initiative launched in 2003 to evaluate biomarkers, neuroimaging and neuropsychological status in participants aged 55–90 years, both with and without cognitive concerns. Participants in ADNI received detailed clinical and cognitive assessments. ADNI database was approved by institutional review boards of all participating centers, with informed consent obtained from all participants or their authorized representatives.

Measures

Blood samples were collected in EDTA tubes, processed to produce plasma, and stored at −80 °C until analysis. Analyses were conducted by University of Pennsylvania (Pathology & Laboratory Medicine), ran in batches approximately every four months to ensure consistency and reliability. Plasma p-Tau217 and Aβ42 were quantified using immunoassay reagents from Fujirebio on the Lumipulse G1200 platform. Quality control samples were included in each analytical run, with precision across runs ranging from 6.2 to 9.9 % for pTau217 and 5.1–5.4 % for Aβ42.

Amyloid PET imaging was conducted using [18F] florbetapir (FBP) and [18F] florbetaben (FBB) tracers. PET data were processed by University of California, Berkeley (Helen Wills Neuroscience Institute), using a standardized pipeline that included co-registration to MRI scans, intensity normalization, and calculation of overall amyloid burden based on SUVR (standardized uptake value ratio) of the cortical summary region (i.e. frontal, anterior/posterior cingulate, lateral parietal, and lateral temporal regions). Of note, two normalization approaches were used to calculate SUVR (i.e. using whole cerebellum as the reference region; or using a composite reference region made up of whole cerebellum, brainstem, and eroded subcortical white matter), with ADNI recommending whole cerebellum-normalized SUVR for cross-sectional analyses, and composite-reference-normalized SUVR for longitudinal analyses.

Amyloid PET positivity was determined using established SUVR thresholds specific to each radiotracer (i.e. FBP or FBB) and reference region (i.e. whole cerebellum or composite reference) [22,23]. For the radiotracer of FBP, the positivity threshold was 1.11 for whole cerebellum-normalized SUVR or 0.78 for composite-reference-normalized SUVR. For FBB, the threshold was 1.08 for whole cerebellum-normalized SUVR or 0.74 for composite-reference-normalized SUVR. The thresholds for whole cerebellum-normalized SUVR were previously derived from the upper limit in young controls; while the thresholds for composite-reference-normalized SUVR were derived through linear transformation from whole cerebellum-normalized thresholds. Quality control of PET data was performed through visual inspection by technicians.

Statistical analyses

Prior to analysis, the raw data on p-Tau217 and p-Tau217/Aβ42 ratio were pre-processed using Box-Cox transformation (to normalize the distribution of skewed data) and standardization (to produce z-scores and improve stability during modelling). Of note, Box-Cox transformation is a well-established method for addressing skewed distributions. It identifies the optimal parameter (λ) for a power transformation that stabilizes variance and approximates normality, making the method more robust than other simpler transformations. The transformation is based on the formula:

$$Transformed\ values = \frac{(Raw\ values)^{\lambda} - 1}{\lambda}$$

with $\lambda = -0.2$ for p-Tau217 and p-Tau217/Aβ42 ratio in this study.

Primary analyses were conducted on the full sample ($n = 1039$), using FMM to derive optimal cutoffs for p-Tau217 and p-Tau217/Aβ42 ratio. Analyses were conducted separately for p-Tau217 and p-Tau217/Aβ42 ratio. Models with 1 to 6 latent classes were explored in FMM, allowing for varying variance and covariance structures. The best-fitting model was selected based on the lowest Bayesian Information Criterion (BIC), which balances model complexity and goodness of fit [24]. In the event of similar BIC (i.e. difference <10 points), the more parsimonious model was preferred. Fit indices of evaluated models are presented in Supplementary Materials 1 and 2, with two-class model (equal variance; zero covariance structure) showing the best fit and was thus selected. This two-class model aligns with the hypothesis of two identifiable subpopulations: brain amyloid negative and positive.

FMM generated probability scores reflecting participants' likelihood of belonging to each of the two classes. Participants with class probability ≥80 % were deemed to have reasonably high certainty of belonging to one of the two classes (i.e. test negative or test positive), while those falling in the grey zone between the two classes (i.e. with probability <80 % for both classes) were deemed as 'Indeterminate'. Optimal cutoffs were identified based on the boundaries of the Indeterminate zone. Effectively, this approach classifies participants into test negative, indeterminate, or test positive categories; consistent with the two-cutoff

approach advocated in recent AD literature [6] to enhance test performance and prioritize resources for those requiring further testing.

Secondary analyses were conducted on the subset with available amyloid PET data (n = 711), to validate the performance of FMM-derived cutoffs against amyloid PET positivity. A priori, optimal test statistics were defined as negative predictive value (NPV)≥90 %, positive predictive value (PPV)≥90 %, and proportion of individuals in indeterminate group≤20 % [6]. While sensitivity and specificity were also reported, they were not considered within the optimal criteria for test statistics, given this study's primary focus on deriving population-specific cutoffs rather than generalizing cutoffs across different populations. Test statistics were also compared with those from previously-published cutoffs for plasma p-Tau217 and p-Tau217/Aβ42 ratio on the Lumipulse platform [7–15]. The 95 % confidence intervals (CIs) of test statistics were computed using:

$$Proportion \pm 1.96 \times \sqrt{\frac{Proportion \times (1 - Proportion)}{Denominator\ for\ the\ Proportion}}$$

An exploratory analysis examined the minimum sample size required to estimate optimal cutoffs using FMM. Values of p-Tau217 (and separately, p-Tau217/Aβ42 ratio) were simulated from a bimodal distribution, using mean and standard deviation estimates from the output of FMM in the primary analyses. Based on 1000 bootstrap resampling, the 95 % CIs for optimal cutoffs were computed for sample sizes ranging from 200 to 3000 (in steps of 100). The minimum sample size was indicated by the smallest sample where the 95 % CI was narrower than cutoff ±10 %. This ±10 % margin is a practical rule-of-thumb that has been adopted in prior biomarker studies [21], and reflects a variability that is sufficiently small and less likely to be clinically meaningful [25].

Statistical analyses were conducted in R (version 4.4.1), using 'caret' package for pre-processing [26], 'tidySEM' for FMM [27], and 'boot' for bootstrap resampling [28].

Results

Demographic information of the study participants (n = 1039) is presented in Supplementary Material 3, showing a mean age of 74.2 years and mean education of 16.3 years. Majority were of white ethnicity (82.0 %), with normal cognition (48.4 %) or mild cognitive impairment (32.3 %). Two-third of the participants had amyloid PET data (n = 711; as shown in Supplementary Material 3); these participants were more likely to be younger, female, APOE e4 non-carriers, cognitively unimpaired, and had lower values in plasma p-Tau217 and p-Tau217/AB42 ratio.

Plasma p-Tau217 showed a right-skewed distribution (Fig. 1a), which approximated normality following Box-Cox transformation (Fig. 1b). FMM identified two subpopulations based on the plasma values (Fig. 1c): brain amyloid negative (green density plot) and brain amyloid positive (red density plot). FMM generated probabilities of class membership as depicted in Fig. 1d, with the green line indicating the probability of being brain amyloid negative and the red line indicating brain amyloid positive. The greyed area in Fig. 1d marks the Indeterminate zone, where class membership was less certain (<80 % probability for either class). The boundaries of the greyed area define the FMM-derived cutoffs: values below the lower boundary (corresponding to ≤0.1637 pg/mL) identify test negative, and values above the upper boundary (corresponding to ≥0.2924 pg/mL) identify test positive. Similar results were observed for plasma p-Tau217/Aβ42 ratio (Supplementary Material 4), with corresponding cutoffs of ≤0.0063 for test negative, values between 0.0063–0.0114 for indeterminate, and ≥0.0114 for test positive.

Secondary analyses validated FMM-derived cutoffs against amyloid PET positivity in the subset with available amyloid PET data (n = 711), with the results presented in Table 1. Even without relying on gold standards, FMM-derived cutoffs showed respectable test statistics (indeterminate proportion below 20 %, and NPV and PPV near or above 90 %), albeit with plasma p-Tau217/Aβ42 ratio outperforming plasma p-Tau217. When compared to previously-published cutoffs [7–15], FMM-derived cutoff largely achieved better balance across indeterminate proportion, NPV and PPV, especially for plasma p-Tau217. The cutoff values from FMM were also not dissimilar to ADNI-recommended cutoffs. In contrast, the FDA-approved cutoffs [18] for Lumipulse plasma p-Tau217/Aβ42 ratio performed much poorer, with indeterminate proportion 28.3 % and PPV<90 %.

It is relevant to note that while the FMM-derived cutoffs in the main analyses above were based on probability threshold of ≥80 % (reflecting reasonable certainty for class membership), alternative probability thresholds could also be chosen to balance different trade-offs between indeterminate proportion and NPV/PPV. Supplementary Material 5 further illustrates results with other thresholds – probability threshold of ≥50 % could minimize indeterminate proportion but lower NPV/PPV; while probability thresholds of ≥90 % could maximize NPV/PPV but increase indeterminate proportion.

Exploratory analysis examined the effects of sample size on FMM-derived cutoffs, with the simulation results detailed in Supplementary Materials 6 and 7. As sample size increases, the 95 % CIs of the cutoffs became narrower. A minimum sample size of 900 is required to achieve acceptable 95 % CIs, where maximum variability of the cutoffs is <10 % (i.e. reflecting a variability that is sufficiently small and less likely to be clinically meaningful).

DISCUSSION

This study demonstrated the utility of FMM in deriving population-specific cutoffs for plasma p-Tau217 and p-Tau217/Aβ42 ratio, offering a novel approach that circumvents reliance on traditional gold standards. FMM-derived cutoffs effectively classified participants into brain amyloid negative and positive groups, with an indeterminate zone for cases of less certain classification. These cutoffs demonstrated test performance that matched or surpassed previously-established thresholds, achieving an indeterminate proportion below 20 %, and NPV and PPV near or above 90 %, with plasma p-Tau217/Aβ42 ratio being superior to plasma p-Tau217. Based on simulation, a minimum sample size of 900 is required for reliable estimation of FMM-derived cutoffs.

Recent advancements in anti-amyloid therapies [2,3] have highlighted the relevance of plasma biomarkers, particularly plasma pTau-217 and p-Tau217/Aβ42 ratio [6–16], as accessible and cost-effective tests to identify AD for early intervention [4,5]. However, widespread adoption of plasma pTau-217, particularly outside of tertiary specialist centers and in LMICs, has been constrained by the limited availability of population-specific reference intervals necessary for accurate results interpretation. Current findings highlight the viable solution offered by FMM, which can provide accurate cutoff estimates even in the absence of gold standards, overcoming challenges in obtaining gold standards related to invasive procedures (CSF) or high cost (PET). FMM requires only blood samples from 900 community-representative individuals to derive reliable and valid cutoffs. This approach can produce less biased cutoffs, considering that samples with gold standard data are often difficult to acquire and may not represent the general population. This approach is also more cost-effective than PET, which can be about 10–20 times more expensive than plasma analysis. For the cost of analysing 900 plasma samples, this would only allow for 45–90 PET, which has insufficient statistical power for conventional ROC analysis.

Conventional ROC analysis often maximizes sensitivity and specificity, assuming these metrics are less affected by disease prevalence and are thus more generalizable. However, when specific cutoffs are applied to a population, interpretation within each population often still relies on NPV and PPV [6], which can vary widely with disease prevalence [6] and demographic factors [4,5,19]. As demonstrated by the current findings (Table 1), many of the previously-published ROC-based cutoffs – including the FDA-approved cutoffs [18] – may not necessarily be optimal for the ADNI sample. In contrast, the FMM approach proposes

Table 1
Comparison of FMM-derived cutoffs with previously known cutoffs, in the subset of participants with amyloid PET data (n = 711). The FMM-derived cutoffs are highlighted in bold.

Source of biomarker cutoff	Lower cutoff [b]	Upper cutoff [c]	Indeterminate group, % (95 % CI) [d]	Amyloid PET positive (Based on whole cerebellum-normalized SUVR) [a]				Amyloid PET positive (Based on composite-reference-normalized SUVR) [a]			
				NPV, % (95 % CI) [d]	PPV, % (95 % CI) [d]	Sensitivity, % (95 % CI) [e]	Specificity, % (95 % CI) [e]	NPV, % (95 % CI) [d]	PPV, % (95 % CI) [d]	Sensitivity, % (95 % CI) [e]	Specificity, % (95 % CI) [e]
Plasma p-Tau217 (in pg/mL unit)											
FMM-derived cutoff (current study)	**≤0.164**	**≥0.292**	**15.6 (12.9–18.3)**	**87.5 (84.2–90.8)**	**93.0 (89.6–96.4)**	**80.6 (75.7–85.6)**	**95.7 (93.6–97.8)**	**91.7 (88.9–94.4)**	**92.6 (89.0–96.1)**	**86.1 (81.7–90.6)**	**95.7 (93.6–97.7)**
Sarto 2025 [f]	≤0.184	≥0.354	15.0 (12.4–17.7)	85.4 (82.0–88.8)	94.7 (91.4–97.9)	74.4 (68.8–79.9)	97.3 (95.6–98.9)	89.2 (86.2–92.2)	93.6 (90.1–97.1)	79.5 (74.2–84.9)	96.9 (95.1–98.6)
Dyer 2024 [f]	≤0.252	≥0.443	14.5 (11.9–17.1)	80.0 (76.4–83.7)	94.2 (90.2–98.1)	57.8 (51.4–64.3)	97.9 (96.5–99.3)	84.3 (81.0–87.6)	92.7 (88.3–97.1)	63.2 (56.5–69.9)	97.5 (96.0–99.0)
Pozzi 2025 [f]	≤0.124	≥0.328	30.9 (27.5–34.3)	91.8 (88.7–94.9)	93.9 (90.6–97.3)	88.6 (84.3–92.9)	95.7 (93.4–98.1)	95.9 (93.6–98.2)	93.4 (90.0–96.9)	93.9 (90.6–97.2)	95.6 (93.2–97.9)
Feizpour 2024 [f]	<0.140	>0.230	16.9 (14.1–19.6)	90.2 (87.0–93.4)	89.8 (86.1–93.5)	87.4 (83.4–91.4)	92.1 (89.2–95.0)	93.8 (91.2–96.3)	89.0 (85.2–92.9)	91.5 (88.1–95)	91.8 (88.9–94.7)
Wang 2024 (cohort 1) [f]	≤0.230	≥0.514	20.3 (17.3–23.2)	81.6 (78.0–85.1)	93.7 (89.2–98.2)	55.3 (48.2–62.4)	98.2 (96.8–99.5)	86.0 (82.8–89.2)	91.9 (86.8–97.0)	61.4 (54.0–68.9)	97.8 (96.3–99.2)
Wang 2024 (cohort 2) [f]	≤0.086	≥0.197	37.1 (33.6–40.7)	95.3 (92.1–98.5)	87.0 (83.0–91)	96.8 (94.6–99.0)	81.8 (76.4–87.2)	98.2 (96.3–100)	85.6 (81.4–89.7)	98.8 (97.3–100.2)	80.7 (75.3–86.1)
Martinez-Dubarbie 2025 [f]	≤0.133	≥0.252	21.8 (18.8–24.8)	90.8 (87.6–94.0)	90.9 (87.2–94.5)	88.3 (84.3–92.3)	92.9 (90.0–95.7)	94.9 (92.5–97.3)	90.0 (86.3–93.8)	93.1 (89.9–96.4)	92.6 (89.7–95.4)
Arranz 2024 [f]	≤0.187	≥0.386	17.7 (14.9–20.5)	84.6 (81.1–88.0)	95.1 (91.8–98.4)	70.6 (64.6–76.6)	97.8 (96.3–99.3)	88.6 (85.6–91.6)	93.9 (90.2–97.6)	76.2 (70.4–82.1)	97.4 (95.8–99)
Figdore 2024 [f]	≤0.185	>0.324	13.1 (10.6–15.6)	85.0 (81.5–88.4)	94.0 (90.7–97.3)	74.8 (69.4–80.2)	96.7 (94.9–98.6)	88.8 (85.8–91.8)	93.5 (90.0–96.9)	79.8 (74.7–85)	96.6 (94.8–98.4)
Palmqvist 2025 [f]	<0.220	>0.340	9.7 (7.5–11.9)	82.4 (78.9–85.9)	94.3 (91.0–97.6)	69.7 (64.2–75.3)	97.1 (95.4–98.8)	86.4 (83.2–89.6)	93.3 (89.7–96.8)	74.7 (69.2–80.2)	96.8 (95.0–98.5)
ADNI-recommended cutoff [g]	≤0.128	≥0.300	27.7 (24.4–31.0)	91.4 (88.2–94.6)	93.4 (90.1–96.7)	88.4 (84.2–92.6)	95.2 (92.7–97.6)	95.4 (93.0–97.7)	92.9 (89.5–96.4)	93.4 (90.0–96.7)	95 0.0 (92.6–97.5)
Plasma p-Tau217 / Aβ42 ratio											
FMM-derived cutoff (current study)	**≤0.0063**	**≥0.0114**	**15.8 (13.1–18.4)**	**90.0 (87.0–93.0)**	**94.0 (90.9–97.2)**	**84.4 (79.8–88.9)**	**96.3 (94.4–98.3)**	**93.7 (91.3–96.1)**	**93.1 (89.8–96.5)**	**89.4 (85.4–93.4)**	**96.0 (94.0–98.0)**
Wang 2024 (cohort 1) [f]	<0.010	≥0.018	13.4 (10.9–15.9)	81.0 (77.4–84.5)	92.3 (87.9–96.7)	59.5 (53.0–65.9)	97.2 (95.6–98.8)	85.2 (82.0–88.4)	92.3 (87.9–96.7)	65.3 (58.8–71.9)	97.3 (95.8–98.9)
Wang 2024 (cohort 2) [f]	≤0.005	≥0.009	19.5 (16.6–22.5)	94.0 (91.4–96.6)	92.2 (88.9–95.5)	92.5 (89.3–95.8)	93.7 (91.0–96.4)	96.8 (94.9–98.8)	91.4 (88.0–94.8)	95.9 (93.4–98.4)	93.3 (90.6–96)
Martinez-Dubarbie 2025 [f]	≤0.006	≥0.008	9.4 (7.3–11.6)	91.1 (88.2–94.0)	91.2 (87.8–94.6)	88.3 (84.5–92.0)	93.4 (90.8–95.9)	94.1 (91.7–96.5)	90.5 (87.0–94.0)	91.8 (88.5–95.1)	93.1 (90.5–95.6)
ADNI-recommended cutoff [g]	≤0.0055	≥0.0086	14.9 (12.3–17.5)	93.1 (90.4–95.7)	91.9 (88.6–95.2)	90.8 (87.3–94.3)	93.9 (91.3–96.4)	96.0 (93.9–98)	91.1 (87.7–94.6)	94.4 (91.5–97.3)	93.5 (91.0–96.1)
FDA-approved cutoff [h]	≤0.00370	≥0.00738	28.3 (25.0–31.6)	95.0 (92.1–97.9)	89.0 (85.4–92.6)	95.9 (93.6–98.3)	86.7 (82.4–91.0)	97.7 (95.7–99.7)	86.9 (83.1–90.8)	98.1 (96.4–99.7)	84.9 (80.5–89.3)

FMM, Finite Mixture Modelling; PET, positron emission tomography; SUVR, standardized uptake value ratio; NPV, negative predictive value; PPV, positive predictive value; ADNI, Alzheimer's Disease Neuroimaging Initiative; FDA, Food and Drug Administration.

FMM, Finite Mixture Modelling; PET, positron emission tomography; SUVR, standardized uptake value ratio; NPV, negative predictive value; PPV, positive predictive value; ADNI, Alzheimer's Disease Neuroimaging Initiative.

[a] The ADNI database provides two distinct criteria to define amyloid PET positivity, depending on the choice of reference region when computing SUVR (i.e. using whole cerebellum as the reference region; or using a composite reference region made up of whole cerebellum, brainstem, and eroded subcortical white matter); with the whole cerebellum-normalized SUVR recommended for cross-sectional analyses, and the composite-reference-normalized SUVR for longitudinal analyses.

[b] Lower cutoff identifies those who not likely to be brain amyloid positive.

[c] Upper cutoff identifies those who are likely to be brain amyloid positive.

[d] Optimal test statistics were defined as: indeterminate group≤20 %, NPV≥90 %, and PPV ≥90 %.

[e] While sensitivity and specificity were also reported, they were not considered within the optimal criteria for test statistics, given this study's primary focus on deriving population-specific cutoffs rather than generalizing cutoffs across different populations.

[f] Previously-published cutoffs for plasma p-Tau217 and p-Tau217/Aβ42 ratio on the Lumipulse platform.[7–15] When multiple cutoffs were reported in a study, the cutoff with indeterminate group≤20 % was selected for use in the current comparison.

[g] The provisional cutoffs were recommended by the Biomarker Core of ADNI, based on initial validation in the University of Pennsylvania's Alzheimer's Disease Research Center cohort involving 210 white and 80 black participants.

[h] The official cutoffs approved by FDA for Lumipulse plasma p-Tau217/Aβ42 ratio, based on validation in 499 individuals from USA and Europe.[18]

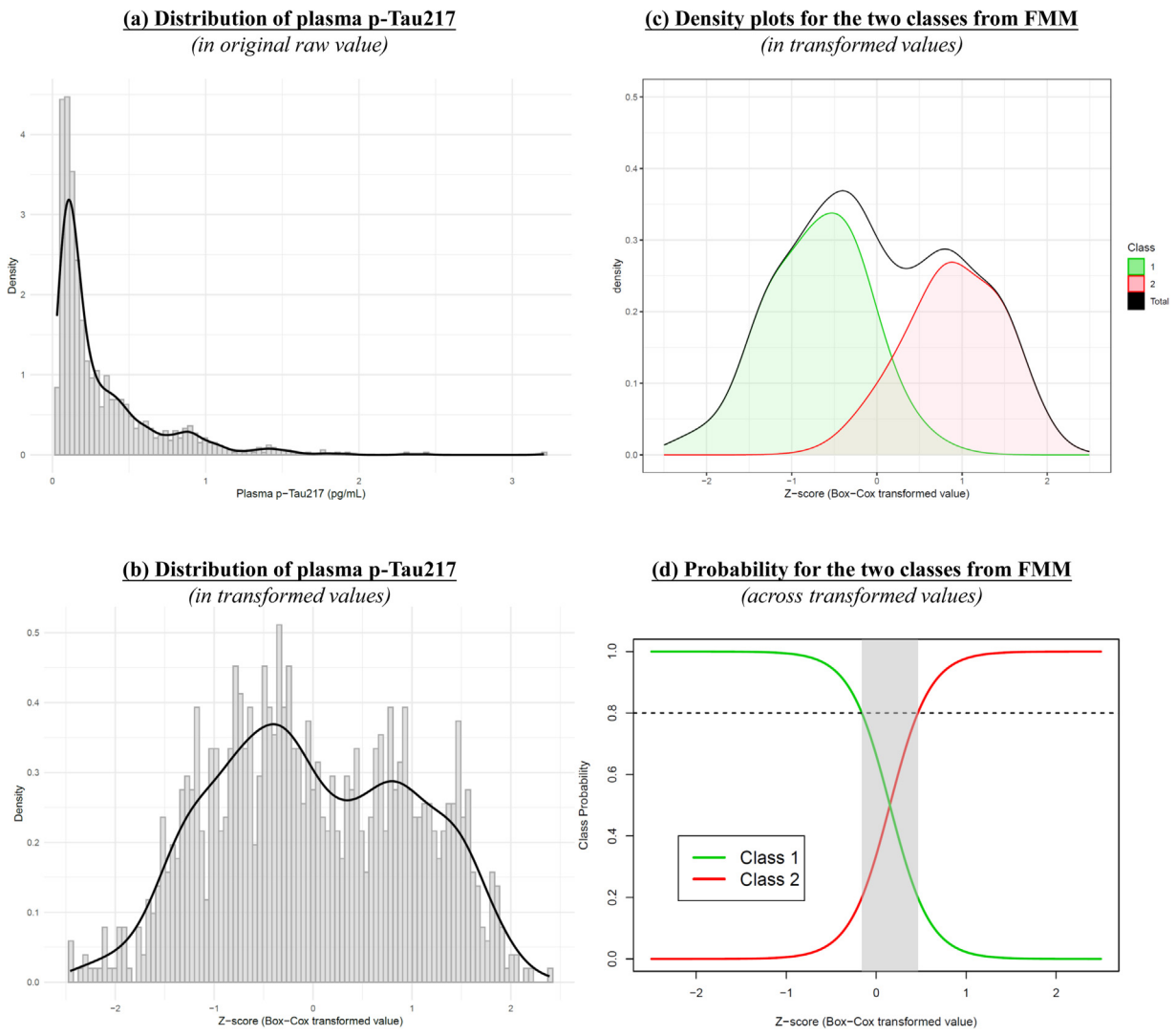

Fig. 1. Distribution of plasma p-Tau217 in the full sample (n = 1039), and finite mixture modelling to derive the optimal cutoffs.
FMM, finite mixture modelling.
Note: In figure (c), the green plot represents the distribution of plasma p-Tau217 (in Box-Cox transformed values) for those who were likely to be brain amyloid negative; while the red plot represents the distribution for those who were likely to be brain amyloid positive. In figure (d), the green line reflects the probability of being brain amyloid negative and the red line reflects the probability of being brain amyloid positive, across the values of plasma p-Tau217 (in Box-Cox transformed values). The greyed area indicates the biomarker range where class membership was less certain (i.e. individuals within this range had <80 % probability of belonging to any class).

independent analysis in each population, using a probabilistic method to directly account for unique population characteristics, thus maximizing NPV/PPV and minimizing the indeterminate group. This approach produces reference intervals that are more tailored and population-specific than those derived from conventional ROC analysis, enhancing accurate identification of brain amyloid positivity for early intervention. A summary of the key findings from this study is presented in Table 2.

Several limitations are notable. First, the subset of participants with amyloid PET differed distinctly from those without (Supplementary Material 3). This reinforces the relevance of current study, highlighting that samples with gold standards may not represent the general population and that FMM can be a less biased approach to derive cutoffs in population-representative samples. However, this also serves as a reminder that findings from the secondary analyses (i.e. validation of cutoffs in subset with amyloid PET) should be interpreted as a general indication of test performance, rather than a true reflection of real-world performance in the general population. Second, the FMM-derived cutoffs were based on plasma p-Tau217 from the Lumipulse platform. They may not be applicable to the other platforms, which would require separate FMM analyses. Third, the ADNI cohort predominantly comprised highly educated White individuals recruited in research settings. Hence, the cutoffs derived in this study may not be applicable to other populations, and would require separate FMM analyses and local recalibration to ensure accuracy.

In conclusion, this study demonstrated the effectiveness of a modelling approach for estimating plasma p-Tau217 cutoffs without reliance on gold standards. This approach simplifies the determination of population-specific reference intervals, facilitating accurate result interpretation and supporting wider adoption of plasma p-Tau217 in community settings and LMICs where gold standards may be unavailable.

FUNDING

TML is supported by the Singapore Ministry of Health's National Medical Research Council (grant numbers: HCSAINV23jul-0001, NMRC/CG2/005e/2022-SGH, MOH-SEEDFD22apr-0001). The funding sources had no involvement in any part of the project.

Table 2
A summary of the key findings from the current study.

Challenges in conventional ROC analysis for cutoff determination	Potential solution offered by FMM
ROC analysis requires gold standards, which may not be available in community settings due to invasive procedures (CSF) or high cost (PET).	FMM can accurately estimate optimal cutoffs with relying on gold standards.
ROC analysis uses samples with gold standards which may not represent the general population, potentially introducing bias and reducing generalizability.	FMM only requires blood samples from 900 representative individuals to derive reliable and valid cutoffs, which is more feasible in community settings
ROC analysis maximizes sensitivity and specificity, assuming these metrics are less affected by disease prevalence and thus more generalizable. Yet, interpretation within each population often still relies on NPV and PPV, which vary widely with disease prevalence and demographic factors.	FMM uses a probabilistic approach to directly account for unique characteristics within each population, maximizing NPV/PPV and minimizing indeterminate group.

ROC, receiver operating characteristic curve; CSF, cerebrospinal fluid; PET, positron emission tomography; NPV, negative predictive value; PPV, positive predictive value; FMM, Finite Mixture Modelling.

ETHICAL standards

The ADNI database was approved by institutional review boards of all participating centers, and written informed consent was obtained from all participants or their authorized representatives.

Declaration of competing interest

The authors declare the following financial interests/personal relationships which may be considered as potential competing interests: Tau Ming Liew reports financial support was provided by National Medical Research Council. Tau Ming Liew reports a relationship with Lundbeck LLC that includes: consulting or advisory. Tau Ming Liew reports a relationship with Eisai Inc that includes: consulting or advisory. If there are other authors, they declare that they have no known competing financial interests or personal relationships that could have appeared to influence the work reported in this paper.

CRediT authorship contribution statement

Tau Ming Liew: Writing – review & editing, Writing – original draft, Visualization, Validation, Supervision, Software, Methodology, Investigation, Formal analysis, Data curation, Conceptualization.

ACKNOWLEDGEMENTS

Data collection and sharing for the Alzheimer's Disease Neuroimaging Initiative (ADNI) is funded by the National Institute on Aging (National Institutes of Health Grant U19AG024904). The grantee organization is the Northern California Institute for Research and Education. In the past, ADNI has also received funding from the National Institute of Biomedical Imaging and Bioengineering, the Canadian Institutes of Health Research, and private sector contributions through the Foundation for the National Institutes of Health (FNIH) including generous contributions from the following: AbbVie, Alzheimer's Association; Alzheimer's Drug Discovery Foundation; Araclon Biotech; BioClinica, Inc.; Biogen; Bristol-Myers Squibb Company; CereSpir, Inc.; Cogstate; Eisai Inc.; Elan Pharmaceuticals, Inc.; Eli Lilly and Company; EuroImmun; F. Hoffmann-La Roche Ltd and its affiliated company Genentech, Inc.; Fujirebio; GE Healthcare; IXICO Ltd.; Janssen Alzheimer Immunotherapy Research & Development, LLC.; Johnson & Johnson Pharmaceutical Research & Development LLC.; Lumosity; Lundbeck; Merck & Co., Inc.; Meso Scale Diagnostics, LLC.; NeuroRx Research; Neurotrack Technologies; Novartis Pharmaceuticals Corporation; Pfizer Inc.; Piramal Imaging; Servier; Takeda Pharmaceutical Company; and Transition Therapeutics.

Supplementary materials

Supplementary material associated with this article can be found, in the online version, at doi:10.1016/j.tjpad.2025.100264.

References

[1] Hansson O, Blennow K, Zetterberg H, Dage J. Blood biomarkers for Alzheimer's disease in clinical practice and trials. Nat Aging 2023;3(5):506–19.
[2] van Dyck CH, Swanson CJ, Aisen P, et al. Lecanemab in early Alzheimer's Disease. N Engl J Med 2023;388(1):9–21.
[3] Sims JR, Zimmer JA, Evans CD, et al. Donanemab in early symptomatic Alzheimer disease: the TRAILBLAZER-ALZ 2 randomized clinical trial. Jama 2023;330(6):512–27.
[4] Schöll M, Verberk IMW, Del Campo M, et al. Challenges in the practical implementation of blood biomarkers for Alzheimer's disease. Lancet Healthy Longev 2024;5(10):100630.
[5] Schöll M, Vrillon A, Ikeuchi T, et al. Cutting through the noise: a narrative review of Alzheimer's disease plasma biomarkers for routine clinical use. J Prev Alzheimers Dis 2025:100056.
[6] Schindler SE, Galasko D, Pereira AC, et al. Acceptable performance of blood biomarker tests of amyloid pathology - recommendations from the Global CEO Initiative on Alzheimer's Disease. Nat Rev Neurol 2024;20(7):426–39.
[7] Sarto J, Esteller-Gauxax D, Guillén N, et al. Accuracy and clinical applicability of plasma tau 181 and 217 for Alzheimer's disease diagnosis in a memory clinic cohort. J Neurol 2025;272(2):160.
[8] Pozzi FE, Conti E, Remoli G, et al. Core blood biomarkers of Alzheimer's disease: a single-center real-world performance study. J Prev Alzheimers Dis 2025;12(2):100027.
[9] Feizpour A, Doecke JD, Doré V, et al. Detection and staging of Alzheimer's disease by plasma pTau217 on a high throughput immunoassay platform. EBioMedicine 2024;109:105405.
[10] Wang J, Huang S, Lan G, et al. Diagnostic accuracy of plasma p-tau217/Aβ42 for Alzheimer's disease in clinical and community cohorts. Alzheimers Dement 2025;21(3):e70038.
[11] Martínez-Dubarbie F, Guerra-Ruiz A, López-García S, et al. Diagnostic performance of plasma p-tau217 in a memory clinic cohort using the Lumipulse automated platform. Alzheimers Res Ther 2025;17(1):68.
[12] Arranz J, Zhu N, Rubio-Guerra S, et al. Diagnostic performance of plasma pTau(217), pTau(181), aβ(1-42) and aβ(1-40) in the LUMIPULSE automated platform for the detection of Alzheimer disease. Alzheimers Res Ther 2024;16(1):139.
[13] Figdore DJ, Griswold M, Bornhorst JA, et al. Optimizing cutpoints for clinical interpretation of brain amyloid status using plasma p-tau217 immunoassays. Alzheimers Dement 2024;20(9):6506–16.
[14] Palmqvist S, Warmenhoven N, Anastasi F, et al. Plasma phospho-tau217 for Alzheimer's disease diagnosis in primary and secondary care using a fully automated platform. Nat Med 2025.
[15] Dyer AH, Dunne J, Dolphin H, et al. Clinical performance of the fully automated Lumipulse plasma p-tau217 assay in mild cognitive impairment and mild dementia. Alzheimers Dement (Amst) 2025;17(1):e70080.
[16] Food and Drug Administration. FDA clears first blood test used in diagnosing Alzheimer's disease. https://www.fda.gov/news-events/press-announcements/fda-clears-first-blood-test-used-diagnosing-alzheimers-disease. Published 2025. Accessed 21 May 2025.
[17] Catania M, Battipaglia C, Perego A, et al. Exploring the ability of plasma pTau217, pTau181 and beta-amyloid in mirroring cerebrospinal fluid biomarker profile of Mild Cognitive Impairment by the fully automated Lumipulse(®) platform. Fluids Barriers CNS 2025;22(1):9.
[18] U.S. Food and Drug Administration 510(k) Premarket notification. US Food and Drug Administration; 2025 https://www.accessdata.fda.gov/scripts/cdrh/cfdocs/cfpmn/pmn.cfm?ID=K242706 PublishedAccessed 18 June 2025.
[19] Nayyar A, Li ML, Sotelo V, et al. Influence of cognitive impairment and race on plasma p-tau(217) in two diverse cohorts. Alzheimers Dement 2025;21(2):e14585.
[20] Kang T, Yoo J, Jekarl DW, et al. Indirect method for estimation of reference intervals of inflammatory markers. Ann Lab Med 2023;43(1):55–63.
[21] Bertens D, Tijms BM, Scheltens P, Teunissen CE, Visser PJ. Unbiased estimates of cerebrospinal fluid β-amyloid 1-42 cutoffs in a large memory clinic population. Alzheimers Res Ther 2017;9(1):8.
[22] Joshi AD, Pontecorvo MJ, Clark CM, et al. Performance characteristics of amyloid PET with florbetapir F 18 in patients with alzheimer's disease and cognitively normal subjects. J Nucl Med 2012;53(3):378–84.

[23] Royse SK, Minhas DS, Lopresti BJ, et al. Validation of amyloid PET positivity thresholds in centiloids: a multisite PET study approach. Alzheimers Res Ther 2021;13(1):99.
[24] Nylund KL, Asparouhov T, Muthén BO. Deciding on the number of classes in latent class analysis and growth mixture modeling: a Monte Carlo simulation study. Structural Equation Modeling: A Multidisciplinary Journal 2007;14(4):535–569.
[25] Liew TM, Yap P, Luo N, Hia SB, Koh GC, Tai BC. Detecting pre-death grief in family caregivers of persons with dementia: measurement equivalence of the Mandarin-chinese version of Marwit-Meuser Caregiver Grief Inventory. BMC Geriatr 2018;18(1):114.
[26] Kuhn M. Building predictive models in R using the caret package. J Stat Softw 2008;28(5):1–26.
[27] Van Lissa C.J. tidySEM: tidy structural equation modeling. R package version 0.2.1. https://github.com/cjvanlissa/tidySEM/. Published 2019. Accessed 25 Feb 2025.
[28] Canty A., Ripley B. boot: bootstrap R (S-Plus) functions. R package version 1.3-31. https://cran.r-project.org/web/packages/boot/index.html. Published 2024. Accessed 25 Feb 2025.